Available online at www.sciencedirect.com
SCIENCE DIRECT®

Journal of the European Ceramic Society 24 (2004) 1425–1429

www.elsevier.com/locate/jeurceramsoc

Defect properties of langasite and effects on BAW gas sensor performance at high temperatures

Huankiat Seh[a,*], Harry L. Tuller[a], Holger Fritze[b]

[a]*Department of Materials Science and Engineering, Massachusetts Institute of Technology, Room 13-4010, 77 Massachusetts Ave, Cambridge, MA 02139, USA*

[b]*Department of Physics, Metallurgy and Materials Science, Technische Universität Clausthal, D-38678 Clausthal-Zellerfeld, Germany*

Abstract

The electrical and defect properties of langasite ($La_3Ga_5SiO_{14}$) were studied as a function of temperature, oxygen partial pressure and dopants in order to characterize its electrical behavior in relation to its performance as a bulk acoustic wave (BAW) gas sensor operating at elevated temperatures. Undoped, 5%–Nb donor doped, and 1%–Sr acceptor doped langasite specimens were studied. A defect model, shown to be consistent with experimental observations, was used to extract key defect parameters for the system. Implications for device operation are discussed.

Keywords: Electrical properties; Impedance; Langasite; Sensors

1. Introduction

Bulk acoustic wave (BAW) devices exhibit exceptional mass sensitivity. The quartz crystal microbalance (QCM) is widely used to detect film thickness changes down to the order of monolayers. Such device can be utilized as gas sensors by depositing films with selectivity to specific gaseous species. As gas molecules adsorb on the film surface, they induce a mass change which is then detected via a shift in the resonant frequency of the device. While QCMs are relatively inexpensive and readily available, quartz has a destructive phase transformation at ~573 °C, and cannot therefore be operated at elevated temperatures. To overcome this limitation, our group has undertaken the investigation of alternative materials, focusing initially on langasite ($La_3Ga_5SiO_{14}$), which exhibits no phase transitions up to its melting point of 1470 °C[1] and for which high quality crystals are available.[2,3]

Langasite has increasingly drawn the attention of SAW and BAW device designers due to its superior properties compared with quartz.[3–7] Many have reported its successful use in filters, and even at high temperature.[8] In our initial investigations, a langasite bulk acoustic wave device was successfully operated as a microbalance to temperatures as high as 900 °C. By adding a TiO_2 film onto the langasite resonator, sensitivity to hydrogen gas was demonstrated[9–11] and means for minimizing temperature cross sensitivity was presented.[12] In these studies, a general drop in quality factor Q was observed with increasing temperature, resulting in reduced resolution in mass-induced frequency shifts. This drop in Q value is suspected, in large part, to be due to increasing electrical losses induced by corresponding increases in bulk conductivity of langasite. In a preliminary investigation of the electrical and transport properties of langasite, the results pointed to mixed ionic and electronic conduction with the overall electrical resistivity, as measured in air, decreasing exponentially with reciprocal temperature with an activation energy on the order of 1 eV.[13]

Since the conductivity of oxides is known to be dependent, in general, on the oxygen partial pressure, dopants and temperature, it is necessary to understand these dependencies before being able to define the operating limits of such sensors. Consequently, in this work, we present the results of an investigation of the bulk conductivity of langasite as function of temperature, and oxygen partial pressure and initial results on the effects of dopants. These results enable the mapping of iso-conductivity lines, and thereby provide a guide to the operating limits for acoustic wave gas sensors fabricated from

* Corresponding author. Tel.: +1-617-253 2364; fax: +1-617-258 5748.

E-mail address: huankiat@mit.edu (H. Seh).

0955-2219/$ - see front matter © 2003 Elsevier Ltd. All rights reserved.
doi:10.1016/S0955-2219(03)00464-3

langasite. These results also provide key information needed in the derivation of an appropriate defect model which allows for predictive capabilities in optimizing the sensor material. In particular, it would provide guidance on how to select dopants to extend operating limits in terms of temperature and oxygen partial pressure. In this paper, we provide a brief outline of the defect model necessary to explain the observed electrical behavior of langasite. A detailed analysis will be provided in a later paper.

A modified expression for Q has been derived by Fritze and coworkers,[14] and is given by:

$$Q_{\text{modifed}} = \frac{R_p}{\left(R_s^2 + R_s R_p\right)} \sqrt{\frac{L_s}{C_s}} \tag{1}$$

where L_s, C_s and R_s are the inductance, capacitance and resistance of the equivalent series resonant circuit, and R_p is the bulk resistance.

Eq. (1) shows a clear link between R_p and Q. Since Fritze and coworkers[14] had determined that L_s and C_s have only slight dependences on temperature, R_s and R_p should have the dominant influence on Q at high temperatures.

2. Theory

2.1. Defect chemistry

For an acceptor-doped oxide system, the following defect and mass action reactions can be written:
oxidation-reduction:

$$O_o^{\times} \leftrightarrow V_o^{\cdot\cdot} + 2e' + \tfrac{1}{2}O_2 \Rightarrow \left[V_o^{\cdot\cdot}\right] n^2 pO_2^{\frac{1}{2}} = K_R(T) \tag{2}$$

electron-hole generation:

$$\text{null} \leftrightarrow e' + h^{\bullet} \Rightarrow np = K_i(T) \tag{3}$$

electroneutrality:

$$n + \left[Sr'_{La}\right] = 2\left[V_O^{\cdot\cdot}\right] \tag{4}$$

(assuming Sr^{2+} enters the La^{3+} site).

At high pO_2, $[Sr'_{La}]$ is assumed to dominate the left side of Eq. (4) leading to a pO_2-independent ionic conductivity. Substituting Eq. (4) into Eqs. (2) and (3) allows us to solve for the minority carriers n and p. The solutions are found in the right hand column of Table 1. At low pO_2, n overtakes $[Sr'_{La}]$ in Eq. (4). Substituting this approximation for Eq. (4) into Eqs. (2) and (3) results in the solutions shown in the middle column of Table 1.

For a donor-controlled system, Eqs. (2) and (3) still apply. However, the electroneutrality equation becomes:
electroneutrality:

$$n = 2\left[Nb_{Ga}^{\cdot\cdot}\right] + 2\left[V_O^{\cdot\cdot}\right] \tag{5}$$

(assuming Nb^{5+} substitution on a Ga^{3+} site).

Table 1
Defect densities as function of oxygen partial pressure for acceptor-doped system

Electroneutrality	$n = 2[V_O^{\cdot\cdot}]$	$[Sr'_{La}] = 2[V_O^{\cdot\cdot}]$
$n=$	$(2K_R)^{1/3} pO_2^{-1/6}$	$(2K_R)^{1/2}/[Sr'_{La}]^{1/2} pO_2^{-1/4}$
$p=$	$K_i/(2K_R)^{1/3} pO_2^{+1/6}$	$K_i[Sr'_{La}]^{1/2}/(2K_R)^{1/2} pO_2^{+1/4}$
pO_2 range	Low $\leftarrow pO_2 \rightarrow$ High	

Solutions for the key defects in the donor-doped system are found in Table 2 following a similar approach as outlined for the acceptor-doped case above.

3. Experimental

Because single crystal langasite was found to exhibit slow reduction-oxidation kinetics, even at elevated temperatures, in this study we utilized polycrystalline specimens with interconnected porosity. Stoichiometric amounts of lanthanum, gallium and silicon oxide were mixed and ball-milled for approximately 24 h and then pressed into 1 inch diameter pellets. Niobium oxide was added for donor doping and strontium carbonate for acceptor doping. The pellets were fired at 1450 °C in air for 10 h. Densities of approximately 90% were obtained with a grain size on the order of 10 μm. X-ray diffraction showed the material to be langasite with no observable second phases.

Pellets with effective cross sectional area of 6.55 mm^2 and length of 5.6 mm were electroded with platinum using platinum ink. AC complex impedance measurements were conducted using a frequency response analyzer (Solartron 1260). The bulk conductivity values were extracted by fitting the spectra to the appropriate equivalent RC circuits. Samples were heated in a tube furnace to temperatures of 700–1000 °C with the oxygen partial pressure controlled with Ar/O_2 (for high pO_2 range) and CO/CO_2 (for low pO_2 range) gas mixtures.

Table 2
Defect densities as function of oxygen partial pressure for donor-doped system

Electroneutrality	$n = 2[V_O^{\cdot\cdot}]$	$n = 2[Nb_{Ga}^{\cdot\cdot}]$
$n=$	$(2K_R)^{1/3} pO_2^{-1/6}$	pO_2 independent
$p=$	$K_i(2K_R)^{-1/3} pO_2^{+1/6}$	pO_2 independent
pO_2 range	Low $\leftarrow pO2 \rightarrow$ High	

4. Results and discussion

The bulk conductivity of nominally undoped langasite was extracted from the complex impedance plots and plotted in Fig. 1 as function of oxygen partial pressure and temperature. The oxygen partial pressure independent component of the total conductivity was assumed to be ionic, as predicted by the defect model for acceptor doped langasite. At lower pO_2, the conductivity becomes pO_2 dependent. By subtracting the constant ionic conductivity from the total conductivity, it became evident that the electronic component exhibits a $pO_2^{-1/4}$ dependence as predicted in Table 1 for electrons in the acceptor controlled regime.

The intentional addition of the acceptor Sr increased the oxygen independent conductivity by an order of magnitude, suppressed the n-type conductivity and introduced a p-type component with a $pO_2^{+1/4}$ dependence. Fig. 2 shows the enhancement of oxygen ion conductivity due to Sr addition, characterized by activation energies of 0.81 and 1.17 eV for nominally undoped and 1% Sr-doped langasite, respectively.

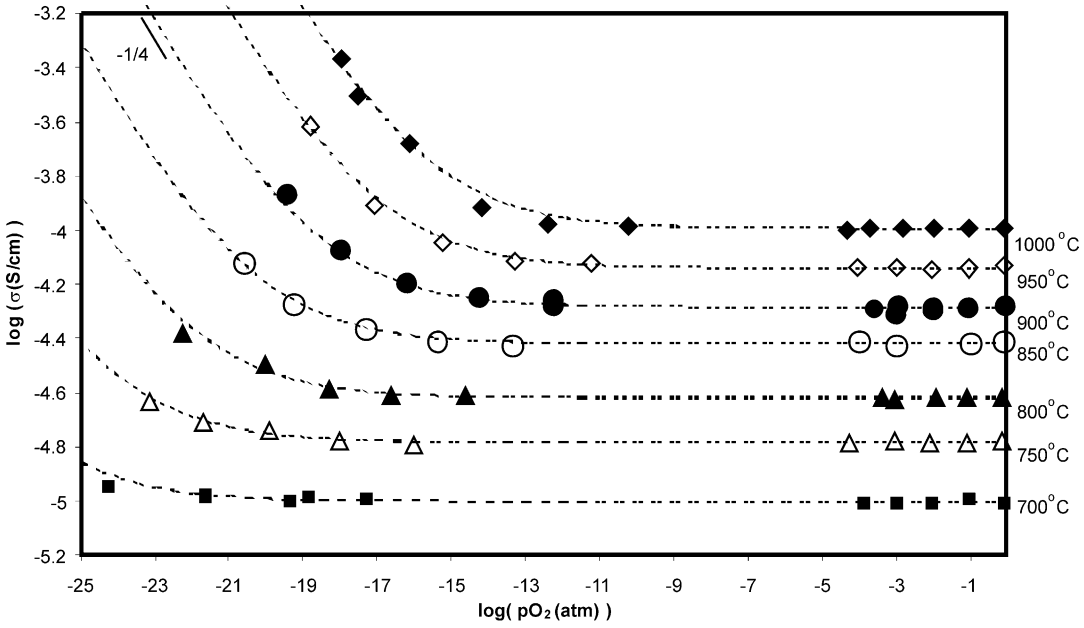

Fig. 1. Bulk electrical conductivity for nominally undoped langsite as function of temperature and oxygen partial pressure.

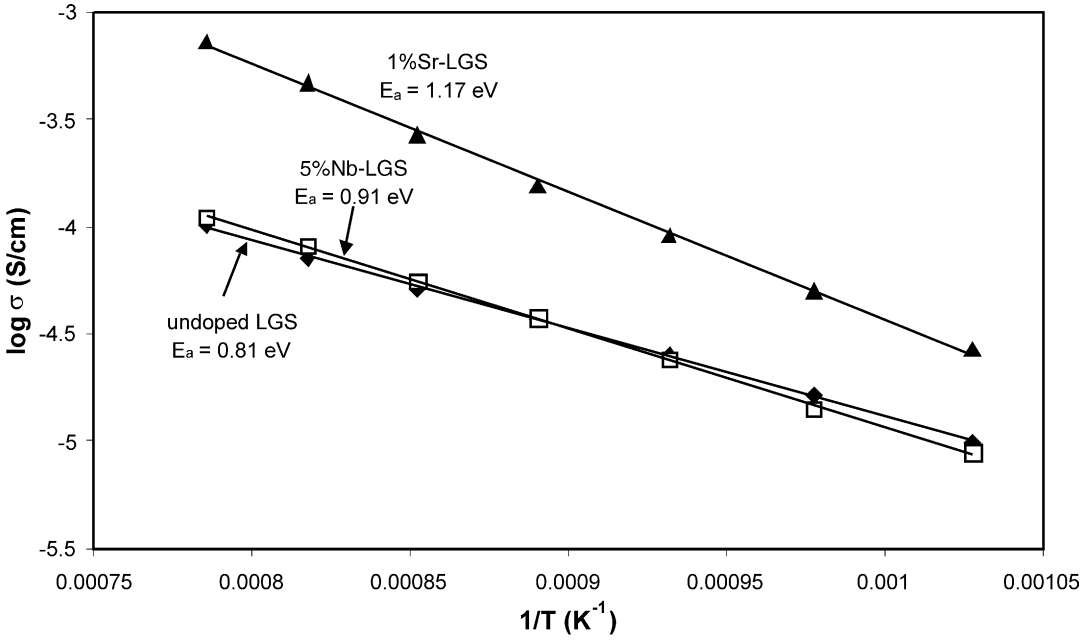

Fig. 2. Conductivity in the oxygen partial pressure independent regime.

These activation energies should reflect the sum of oxygen ion migration and defect-dopant association energies.

The addition of the Nb donor caused a two order of magnitude increase in the *n*-type electronic conductivity compared to undoped langasite (Fig. 3). Furthermore, *n* became proportional to $pO_2^{-1/6}$ rather than $pO_2^{-1/4}$ as for undoped langasite. This suggests that the defect solutions of Table 2 apply, with the middle column applicable at low pO_2 and the right hand column applicable at high pO_2. Indeed we observe a pO_2 independent regime at high pO_2, which in this case is electronic rather than ionic. In this regime, the activation energy is 0.91 eV, which should reflect the ionization energy of Nb and electron mobility activation. Activation energies for

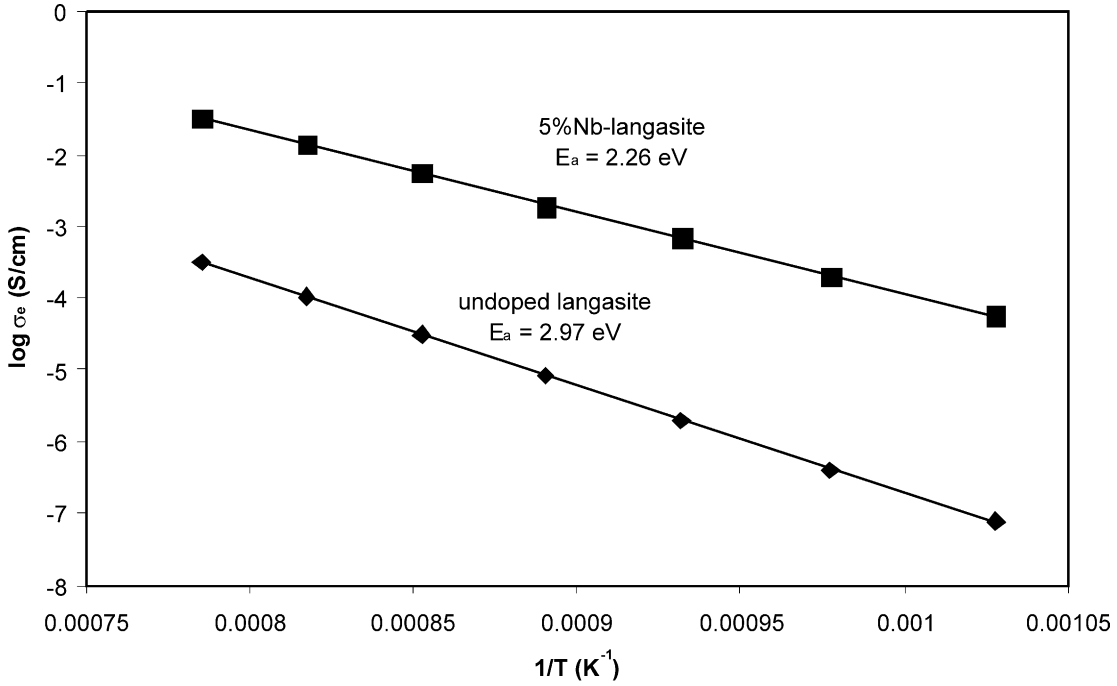

Fig. 3. Electronic conductivity for undoped and 5%–Nb doped langsite evaluated at oxygen partial pressure of 10^{-18} atm.

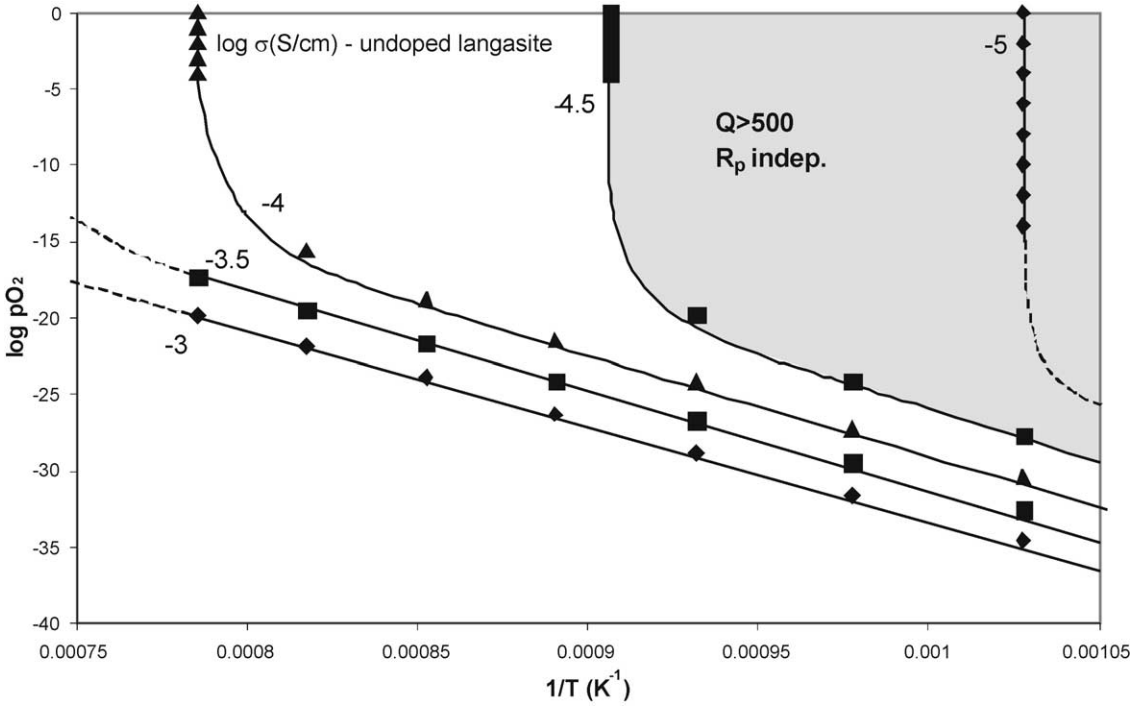

Fig. 4. Iso-conductivity plot for undoped langsite.

the pO_2-dependent conductivities of the undoped and 5% Nb-doped langasite are 2.97 and 2.26 eV, respectively. These two activation energies can be related to the reduction enthalpy defined by K_R in Tables 1 and 2 (i.e. 2.97 eV$\approx E_R/2$; 2.26 eV$\approx E_R/3$)—giving a value of 6–6.8 eV for the reduction enthalpy.

A detailed description of the conductivity data and defect analysis will be published elsewhere. However, from the work presented here, it is clear that dopants can alter the behavior of langasite, and therefore affect the range of temperatures and oxygen partial pressures under which langasite can be operated as a BAW gas sensor, while maintaining an adequate Q value. Using the electrical data from the nominally undoped langasite, we plotted iso-conductivity curves as functions of oxygen partial pressure and temperatures in Fig. 4. Each curve has a corresponding Q value associated with it, and as the conductivity increases, Q decreases. This plot gives information on the possible operating conditions of a langasite resonator. For example, it should be possible to operate to 800 °C from oxygen partial pressures of 1 atm down to $\sim 10^{-12}$ atm while maintaining $Q \geqslant 500$. Using this as a guide, we can utilize dopants to extend the performance area to higher temperatures and/or lower oxygen partial pressure.

5. Conclusion

We have characterized the electrical behavior of langasite polycrystalline samples, both acceptor and donor doped. A defect model was used to describe the electrical behavior of nominally undoped langasite and the dominant sources of electrical conduction contributing to electrical losses. We are now conducting detailed studies and analyses on the effects of dopants on the langasite system to be used to modify the material for optimum performance in BAW-based gas sensors at elevated temperatures.

Acknowledgements

This work was supported by the National Science Foundation under Grant Nos. DMR-9701699, DMR-0228787 and INT-9910012, the Germany Exchange Service (DAAD) and the German Government (BMBF).

References

1. Kaminskii, A. A., Mill, B. V., Khodzhabagyan, G. G., Konstantinova, A. F., Okorochkov, A. I. and Silvestrova, I. M., Investigation of trigonal $(La_{1-x}Nd_x)_3Ga_5SiO_{14}$ crystals: I. Growth and optical properties. *Physica Status Solidi A*, 1983, **80**, 387–398.
2. Chai, B., Lefaucheur, J. L., Ji, Y. Y. and Qiu, H., Growth and evaluation of large size LGS ($La_3Ga_5SiO_{14}$), LGN ($La_3Ga_{5.5}Nb_{0.5}O_{14}$) and LGT ($La_3Ga_{5.5}Ta_{0.5}O_{14}$) single crystals. *IEEE International Frequency Control Symposium*, 1998, 748–760.
3. Mill, B. V. and Pisarevsky, Y. V., Langasite-type materials: from discovery to present state. *IEEE/EIA International Frequency Control Symposium and Exhibition*, 2000, 133–144.
4. Grouzinenko, V. B. and Bezdelkin, V. V., Piezoelectric resonators from $La_3Ga_5SiO_{14}$ (langasite) single crystals. *IEEE Frequency Control Symposium*, 1992, 707–712.
5. Sato, M., Moroishi, K., Ishigami, S., Sakharov, S. A. and Medvedev, A. V., Filter and resonator using langasite. *IEEE International Frequency Control Symposium*, 1996, 379–383.
6. Detaint, J., Zarka, A., Capelle, B., Palmier, D. and Philippot, E., Optimisation of the design of the resonators using the new materials: application to gallium phosphate and langasite. *IEEE International Frequency Control Symposium*, 1997, 566–578.
7. Smythe, R. C., Material and resonator properties of langasite and langatate: a progress report. *IEEE International Frequency Control Symposium*, 1998, 761–765.
8. Honal, M., Fachberger, R., Holzheu, T., Riha, E., Born, E., Pongratz, P. and Bausewein, A., Langasite surface acoustic wave sensors for high temperatures. *IEEE/EIA International Frequency Control Symposium and Exhibition*, 2000, 113–118.
9. Fritze, H. and Tuller, H. L., Langasite for high temperature bulk acoustic wave applications. *Applied Physics Letters*, 2001, **78**, 976–977.
10. Fritze, H., Tuller, H. L., Seh, H. and Borchardt, G., High temperature nanobalance sensor based on langasite. *Sensors and Actuators B*, 2001, **76**, 103–107.
11. Fritze, H., Seh, H., Tuller, H. L. and Borchardt, G., Operation limits of langasite high temperature nanobalances. *Journal of the European Ceramic Society*, 2001, **21**, 1473–1477.
12. Fritze, H. Gas sensor concept based on high temperature piezoelectric materials. Conference paper submitted to "Sensoren und Mess-Systeme", Ludwigsburg, 11–12 March. 2002.
13. Fritze, H., Tuller, H. L., Borchardt, G. and Fukuda, T., High temperature properties of langasite. In *Symposium on Smart Materials—MRS Symposium Proceedings*, ed. R. Gotthardt, K. Uchino, Y. Ito and M. Wun-Fogle. Materials Research Society, Warrendale, PA, 2000, pp. 65–70.
14. Fritze, H., Schneider, O. and Borchardt, G. *High temperature bulk acoustic wave properties of gallium orthophosphate and langasite*. Conference paper submitted to "Sensors and Actuators B: International Meeting on Chemical Sensors", Boston, July 8–10. 2002.